JACS
JOURNAL OF THE AMERICAN CHEMICAL SOCIETY
Article
pubs.acs.org/JACS
Terms of Use

The Membrane Protein LeuT in Micellar Systems: Aggregation Dynamics and Detergent Binding to the S2 Site

George Khelashvili,*[,†] Michael V. LeVine,[†] Lei Shi,[†,‡] Matthias Quick,[§,⊥] Jonathan A. Javitch,[§,∥,⊥] and Harel Weinstein[†,‡]

[†]Department of Physiology and Biophysics, Weill Cornell Medical College of Cornell University (WCMC), New York, New York 10065, United States

[‡]HRH Prince Alwaleed Bin Talal Bin Abdulaziz Alsaud Institute of Computational Biomedicine, Weill Cornell Medical College of Cornell University, New York, New York 10065, United States

Departments of [§]Psychiatry and [∥]Pharmacology, Columbia University College of Physicians & Surgeons, New York, New York 10032, United States

[⊥]Division of Molecular Therapeutics, New York State Psychiatric Institute, New York, New York 10032, United States

Supporting Information

ABSTRACT: Structural and functional properties of integral membrane proteins are often studied in detergent micellar environments (proteomicelles), but how such proteomicelles form and organize is not well understood. This makes it difficult to evaluate the relationship between the properties of the proteins measured in such a detergent-solubilized form and under native conditions. To obtain mechanistic information about this relationship for the leucine transporter (LeuT), a prokaryotic homologue of the mammalian neurotransmitter/sodium symporters (NSSs), we studied the properties of proteomicelles formed by *n*-dodecyl-*β*,D-maltopyranoside (DDM) detergent. Extensive atomistic molecular dynamics simulations of different protein/detergent/water number ratios revealed the formation of a proteomicelle characterized by a constant-sized shell of detergents surrounding LeuT protecting its transmembrane segments from unfavorable hydrophobic/hydrophilic exposure. Regardless of the DDM content in the simulated system, this shell consisted of a constant number of DDM molecules (∼120 measured at a 4 Å cutoff distance from LeuT). In contrast, the overall number of DDMs in the proteomicelle (aggregation number) was found to depend on the detergent concentration, reaching a saturation value of 226±17 DDMs in the highest concentration regime simulated. Remarkably, we found that at high detergent-to-protein ratios we observed two independent ways of DDM penetration into LeuT, both leading to a positioning of the DDM molecule in the second substrate (S2) binding site of LeuT. Consonant with several recent experimental studies demonstrating changes in functional properties of membrane proteins due to detergent, our findings highlight how the environment in which the membrane proteins are examined may affect the outcome and interpretation of their mechanistic features.

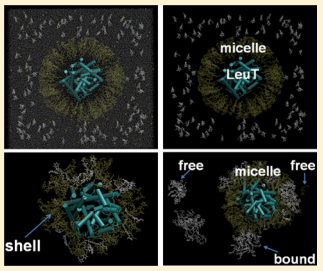

INTRODUCTION

Integral membrane proteins, such as ion channels, receptors, and transporters, perform their vital tasks through complex mechanisms that often involve major structural rearrangements triggered by stimuli such as ligand or substrate binding. The molecular response to the stimuli is propagated across the membrane, connecting the extracellular environment to the interior of the cell. That the membrane environment is involved in the allosteric mechanisms and their regulation is now well-established,[1−3] but the mechanisms by which this environment participate in the observable and measurable activities of the embedded proteins are yielding only slowly to quantitative understanding. In particular, it has become evident that in order to carry out their tasks membrane proteins take advantage of many structural, thermodynamic, and mechanistic properties of the cell plasma membranes and that in turn the lipid membranes respond dynamically to conformational changes in proteins by locally adjusting their lipid composition, bilayer thickness, and/or curvature.[4] Many consequences of such function-dependent cross-talk between proteins and lipids have been identified, including compartmentalization[5,6] and oligomerization[7−13] (often enhanced by specific plasma membrane domains termed rafts[14]), which play central roles in the physiological mechanisms of the cell.

One difficulty in connecting the physiological observations to the rapidly growing information about the detailed structure and dynamic properties of individual membrane protein molecules is that most structural and many functional assays are conducted in non-native environments in which the role of the plasma membrane and its components (i.e., cholesterol and charged lipids) in modulating structural and functional properties of the integral proteins (e.g., ref 15) are not accounted for. Thus, most protein preparation methods for

Received: June 14, 2013
Published: August 27, 2013

   dx.doi.org/10.1021/ja405984v | J. Am. Chem. Soc. 2013, 135, 14266−14275

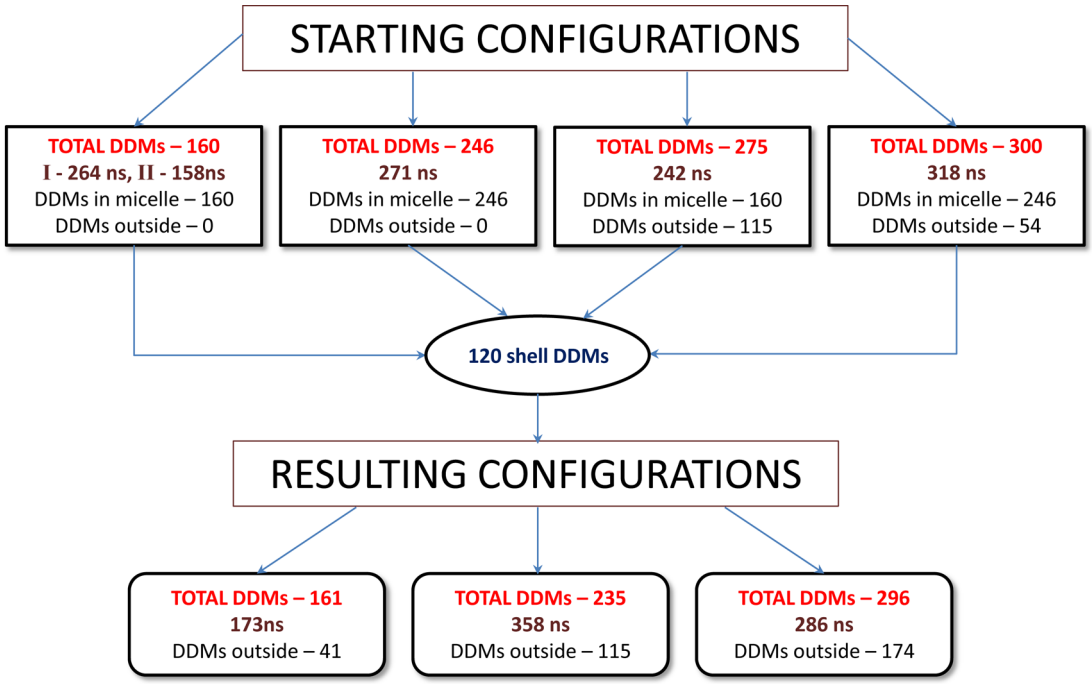

Figure 1. Schematic representation of conditions probed in our all-atom MD simulations of LeuT/detergent complexes: protein-to-detergent number ratios and initial spatial distribution of detergent around LeuT. The first stage of simulations (Starting Configurations) involved LeuT surrounded by a DDM micelle consisting of either 160 or 246 detergent molecules. In addition, different numbers of monomeric DDMs (0, 54, or 115) were placed randomly outside the central protein/detergent micelle (Figure 2A,B). Note that conditions with 160 total DDMs were probed in two separate MD simulations initiated from different random seeds. Because all starting configuration simulations resulted in similar numbers of "shell" DDMs (detergent molecules within 4 Å of a protein, termed shell in Methods), we initiated a second set of simulations (Resulting Configurations) in which LeuT with only its shell of detergents (120 DDMs 4 Å from the protein) was retained (chosen from the representative snapshot from starting configuration trajectories). This protein/detergent complex was then surrounded by randomly placed monomeric DDMs (41, 115, 174 detergents), and new MD trajectories were accumulated. The time durations for each simulation conducted are given in the respective boxes.

studies of integral membrane proteins involve their overexpression, followed by their detergent-mediated extraction from the cell and purification and reconstitution into proteoliposomes.[16] When present in water above certain critical concentrations, the detergents, which have been selected to replace the native environment of these proteins (i.e. the membrane) and possess a relatively large polar headgroup and a short hydrophobic tail, self-assemble in aggregates of positive curvature, termed micelles.[17] In such micelles, the polar headgroups of the detergent are exposed to the aqueous solvent whereas hydrophobic tails face each other and thus mimic the membrane hydrophobic environment for an encapsulated protein while excluding aqueous solvent from the micelle interior. Although micellar aggregates effectively shield hydrophobic trans-membrane (TM) segments of integral proteins from unfavorable polar exposure while bringing polar loop regions into contact with an aqueous phase, they cannot capture all of the complexities of the native plasma membranes.[16] Indeed, several recent studies have provided dramatic demonstrations of changes in functional properties of membrane proteins due to detergent (e.g., refs 18 and 19).

One such class of membrane proteins studied in detergent environments is the family of neurotransmitter/sodium symporters (NSS) that is responsible for the removal of extracellular solutes from the synaptic cleft into the presynaptic nerve terminal.[20] The uptake mechanism is energized by the coupling the transmembrane Na^+ gradient to the uphill transport of the respective substrate. Several X-ray structures of a prokaryotic homologue of NSS, the leucine transporter (LeuT), have identified the centrally located high-affinity substrate binding site, termed the S1 site,[21−28] and two sodium binding sites termed Na1 and Na2. Computational and experimental studies[29] have identified a second high-affinity substrate binding site, the S2 site, located in an extracellular vestibule ∼11 Å above the S1 site that is essential for the transport mechanisms of LeuT. In particular, an allosteric mechanistic model of a Na^+-coupled symport was proposed[29] in which intracellular release of the S1-bound substrate is triggered by the binding of a second substrate molecule in the S2 site.

Remarkably, follow-up studies[19] suggested that experimental conditions and, in particular, a high concentration of *n*-dodecyl-*β*,D-maltopyranoside (DDM) detergent, can obscure the functionally relevant S2 site and result in reduced substrate binding. But the reconstitution of LeuT, previously preincubated with high concentrations of DDM detergent, into *E. coli* membranes, showed a full recovery of functionality for the S2 site.[19] Interestingly, the loss of the S2 site upon detergent treatment appeared to have a concentration threshold in the range of 0.15−0.175% DDM. These experimental results illustrate that the function of integral membrane proteins can be modulated by the experimental preparation and the environment in which the protein is studied. To extrapolate the knowledge gained from the experimental explorations conducted under non-native conditions to mechanisms in vivo, it is necessary to understand on the molecular level how detergent micelles form around proteins and what fundamental changes occur when the protein is surrounded by a detergent

dx.doi.org/10.1021/ja405984v | J. Am. Chem. Soc. 2013, 135, 14266−14275

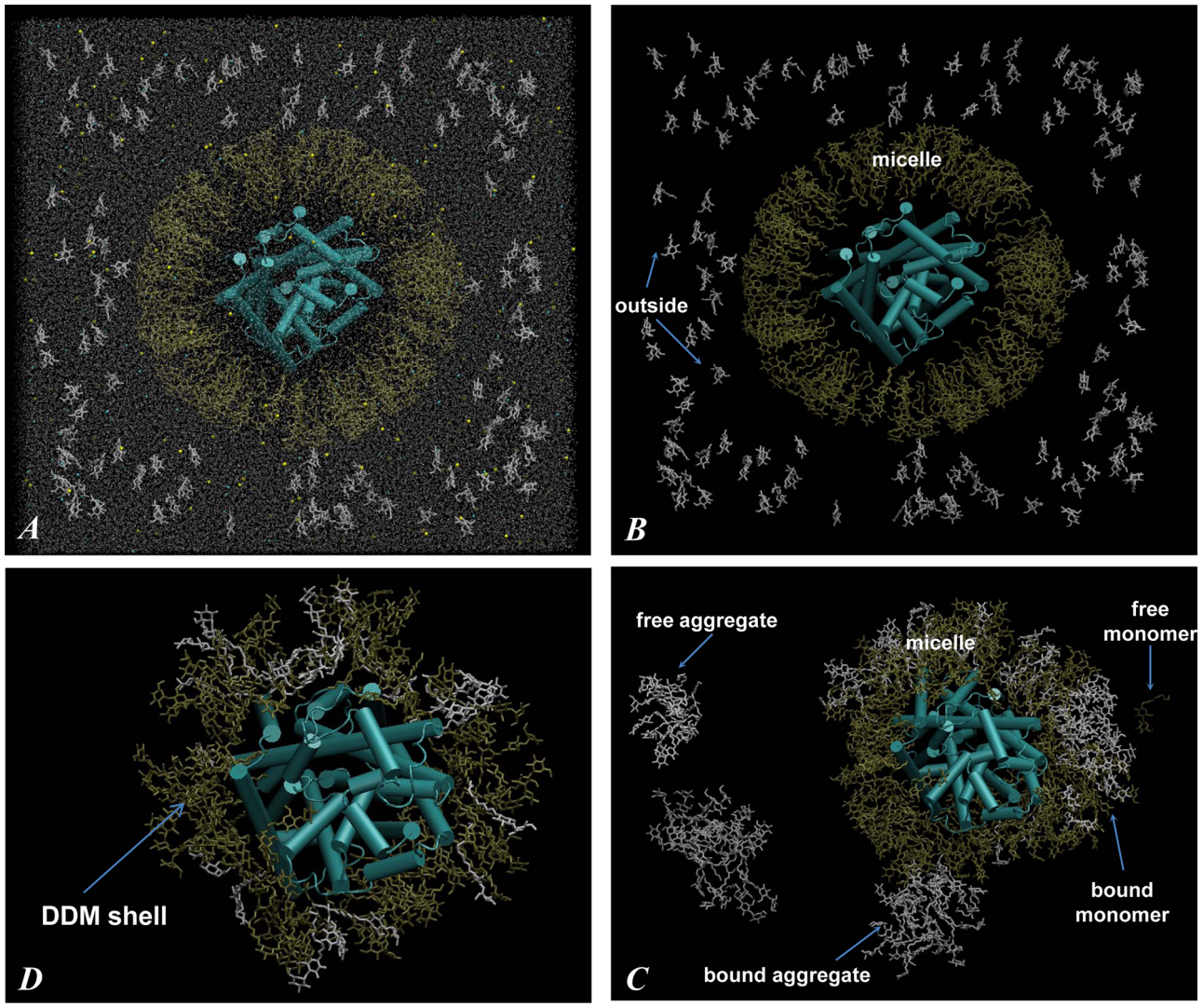

Figure 2. (A) Snapshot of the initial configuration of the 160/115 system (Figure 1, Starting Configurations). The cubic simulation unit box of ∼180 Å linear length contains LeuT protein (in cartoon), DDM detergent molecules (in licorice, 160 DDMs depicted in gold are in the micelle surrounding LeuT and 115 DDMs in white are in monomeric form outside), a water box (silver dots represent water oxygen atoms), and 0.15 M NaCl (yellow and cyan spheres). The leucine ligand bound to the LeuT S1 site and the two Na^+ ions are omitted. (B) Same as in panel A only with water and salt ions removed. (C) Same as in panel B, only after 140 ns of MD simulations. Different types of aggregates (definitions in Methods) are highlighted with arrows and labeled. (D) Final snapshot of the 160/115 system, after 242 ns of simulations, showing only LeuT (cartoon) and shell DDM molecules (within 4 Å of protein) (licorice). Notice strong intermixing of initially micellar (gold) and monomeric (white) DDMs in panels C and D.

micelle. The literature discussing molecular models of detergent/protein interactions (e.g., refs 30−39 and citations therein) has not addressed these fundamental questions in a systematic way.

To point out the shortcomings associated with the interpretation of membrane protein structure and function in experimental environments, we provide here, to our knowledge for the first time, a detailed molecular view of the LeuT protein embedded in DDM detergent micelles formed at different detergent/water/protein ratios. This view is offered from extensive atomistic molecular dynamics (MD) simulations carried out in order to (1) establish the aggregation number of DDM micelles surrounding LeuT, (2) explore the overall organization of the detergent micelle containing the transporter, and (3) obtain molecular-level insight into the nature and consequences of interactions between LeuT and DDM. Analyzing various protein-to-detergent (P/D) number ratios (i.e., from 1:160 to 1:300), we show that the aggregation number of DDM in the micelle that surrounds the transporter is strongly dependent on the P/D ratio. Moreover, the MD simulations of the system at various P/D ratios suggest a mechanism for the dependence of LeuT substrate binding stoichiometry on detergent concentration. Thus, we found that the detergent can penetrate LeuT through two alternative pathways. As a consequence of such penetration, DDM molecules establish long-lasting contacts with several functionally critical residues located in the S2 site of LeuT. Remarkably, we find that the detergent penetration phenotype is determined by the aggregation number of DDM around LeuT so that nontransient DDM insertion is observed only in the high-detergent-concentration regime. These results, discussed here in the light of recent experimental findings suggesting the modulation of LeuT activity by detergent, can explain

dx.doi.org/10.1021/ja405984v | J. Am. Chem. Soc. 2013, 135, 14266−14275

experimentally observed phenotypes caused by the occlusion of the S2 site in LeuT at high detergent concentration.

METHODS

Molecular Constructs. For atomistic molecular dynamics (MD) simulations, we used the X-ray structure of LeuT with the PDB accession code 3GJD.[21] The transporter in this structure is in the occluded state with leucine (Leu) at the S1 primary binding site and the two Na^+ ions bound at Na1 and Na2 sites, respectively. Thus, the structure also contains detergent *n*-octyl-β,D-glucopyranoside (OG) at the S2 binding site. The detergent molecule was removed prior to the simulations, leaving the S2 site empty at the beginning of the MD runs. The LeuT residues that were missing from the 3GJD structure (first four residues on N terminus, last eight residues on C-terminus, and the P132−N133−A134 stretch in the EL2 loop) were added with Modeler.[40] All crystallographic waters were retained in the simulations, and Glu112, Glu287, and Glu419 were treated as protonated.[41,42]

The LeuT model was immersed in a box containing water and DDM detergent molecules. As described in Figure 1 (Starting Configurations) and illustrated in Figure 2, some DDM molecules were initially placed in a spherical micelle formation around LeuT (see below) whereas others were placed randomly as monomers outside this central micelle. The starting conditions were varied with respect to the number of DDMs in the initial micelle and in the monomers. Thus, for the initial set of simulations, the micelle was composed of either 160 or 246 DDM molecules and was surrounded by different numbers of monomeric DDMs (Figure 1). Accordingly, throughout this work, various simulated constructs are given the designation *A*/*B*, where *A* denotes the initial number of DDMs in the central micelle surrounding LeuT (Figure 2) and *B* is the starting number of monomeric detergent molecules outside this micelle.

To build a micelle containing a number *A* of detergent molecules around LeuT, we used a multistep algorithm described in ref 37. According to this procedure, in step 1 *N* pseudoparticles were randomly placed on an imaginary sphere surrounding the protein, excluding areas around intracellular and extracellular parts of LeuT (Figure 2); in step 2, the pseudoparticles were replaced with explicit DDM molecules, oriented with their hydrophobic tails facing the center of LeuT; and in step 3, the imaginary sphere (containing LeuT and all of the DDM molecules) was incrementally shrunk subject to concomitant energy minimization to a final radius of 51 Å. With that, we ensured that in the starting configuration DDM tails were appropriately placed to cover the hydrophobic core of LeuT while leaving hydrophilic regions of the protein exposed to the solvent.

To the box containing the LeuT-detergent micelle complex (proteomicelle) obtained with the procedure described above, we added the desired number of monomeric DDMs (Figures 1 and 2) positioned randomly outside the central micelle, and the system was then solvated with TIP3 waters and ionized with Na^+ and Cl^- to achieve an ionic concentration of 0.15 M. The final simulation box had nearly cubic geometry with a linear dimension of ∼180 Å and contained ∼500 000 atoms. Correspondingly, the detergent concentration was kept above the established critical micelle concentration (cmc) of 0.17 mM for DDM[43,44] in all of the constructs (Table S1 in the Supporting Information).

Molecular Dynamics Simulations. The all-atom MD simulations were done with the NAMD 2.7 package,[45] and the all-atom CHARMM27 force field, with CMAP corrections for proteins[46] and a CHARMM-compatible force-field parameter set for detergents.[47] Molecular constructs were initially equilibrated using a two-phase protocol: (i) short energy minimization was carried out during which protein, water, and ion atoms were fixed and the coordinates of only DDM molecules were allowed to evolve freely and (ii) 1.5-ns-long MD simulations were conducted with the protein backbone harmonically constrained. The constraints were released gradually, in 0.5 ns steps, with decreasing force constants of 1, 0.5, and 0.01 kcal/(mol·Å^2). The equilibration procedure was similar to that implemented by others for MD simulations of protein/micelle complexes (e.g., ref 38).

After the equilibration phase, unbiased MD simulations were carried out. (See Figure 1 for a listing of simulation durations.) Integration steps were 1 fs for the equilibration stage and 2 fs thereafter. The simulations implemented PME for electrostatics interactions[48] and were carried out in an NPT ensemble under isotropic pressure coupling conditions and at 310 K temperature. The Nose-Hoover Langevin piston algorithm[45] was used to control the target P = 1 atm pressure with the Langevin piston period set to 100 fs and the Langevin piston decay set to 50 fs.

Definition of Detergent Aggregates Formed during MD Simulations. As detailed in the Results, the MD simulations led to the spontaneous formation of aggregates of different types (Figure 2C). Accordingly, we distinguished DDM detergents in the following types of aggregates:

Detergent micelles (DMs) − DDMs that are in the central micelle around LeuT;
Bound aggregates (BAs) − DDMs in aggregates that bind to the central micelle;
Bound monomers (BMs) − DDMs that are bound to the central micelle as monomers;
Free aggregates (FAs) − DDMs that are part of aggregates in the solution;
Free monomers (FM) − DDMs that are monomeric in the solution.
DDM shell (shell) − DDMs within 4 Å from LeuT. (See Figure S1 in the Supporting Information for a comparison with the results using alternative definitions of the shell.)

To identify the number of constituent detergent molecules in each type of aggregate defined above, we used an expansion algorithm. Thus, to calculate the number of DDMs in DM, we first identified detergent molecules within 4 Å of LeuT (DDM shell, Figure 2D). Next, we found all DDM molecules within 4 Å of this detergent shell, and such an expansion was repeated until the search failed to identify any new DDM molecules. In this procedure, only the atoms in the hydrophobic tails of detergent molecules were used to differentiate between DDMs in the protein-surrounding micelle from those that are interacting with this micelle via headgroup atoms.

After DM was defined, DDMs in BAs and BMs were counted by selecting detergent molecules whose headgroup atoms were within 5 Å of the DM and building complexes using the expansion algorithm described above. After all bound aggregates were located, the algorithm identified the DDMs in FAs and FMs by building the remaining aggregates in solution. Note that all types of aggregates defined above can, in principle, contain DDM molecules that were initially either part of the central micelle or were monomeric outside the micelle (Figure 2B−D).

The micellar aggregation number is a description of the number of molecules present in a micelle once the CMC has been reached and is defined as the ratio of micelle concentration over the concentration of monomeric detergent.[49] Here, the aggregation number of the LeuT/DDM proteomicelle was calculated as the DM + BA + BM sum. (See above.)

Quantification of Micelle Shape. To quantify the shape of the micelle around LeuT, we calculated the eccentricity E of the *DM* following the procedure implemented in ref 34. To this end, we determined the three principal moments of inertia (I) of an ellipsoid that encloses the non-hydrogen tail atoms of those DDM molecules that were identified as being part of the DM. Using the magnitudes of the smallest principal moment (I_{min}) and of the average of all three moments (I_{av}), we then obtained the eccentricity of the micelle as $E = 1 - (I_{av}/I_{min})$. Note that according to this definition, E = 0 for a perfectly spherical micelle.

Quantification of Detergent Penetration into LeuT from MD Simulations. To quantify the extent of detergent penetration into LeuT in our MD simulations, we monitored the time evolution of selected distance measures from different trajectories. Specifically, because we observed that DDM is inserted into the transporter and binds in the S2 site (see Results), we first screened the residues that have been established from experimental and computational

studies[19,21,24,25,29] to comprise the S2 site in LeuT (see also Discussion): Leu25, Gly26, Leu29, Arg30, Gln34, Tyr107, Tyr108, Ile111, W114, Ala319, Phe320, Phe324, Leu400, and Asp404. We then tracked the minimal distance from these residues to the nearest detergent molecule in different simulations. The penetration of the detergent molecule was observed in different simulations to follow two distinct pathways (see Results), one resulting ultimately in interactions with Arg30 and Gln34 in transmembrane helix 1 (TMH1) of LeuT and the other resulting in interactions with Phe320 in extracellular loop 4 (ECL4) and Leu400 in TMH10. Therefore, we chose to quantify DDM insertion by monitoring the time evolution of the minimal distance (d_{min}) of these four key residues—Arg30, Gln34, Phe320, and Leu400—to the nearest DDM molecule.

In a certain MD trajectory, therefore, a detergent molecule was considered to be fully inserted (complete insertion) into the LeuT S2 site if d_{min} between the detergent and any of the above-mentioned four residues was 3 Å or shorter during at least the last third of the trajectory. If the detergent molecule interacted with either Arg30, Gln34, Phe320, or Leu400 (d_{min} < 3 Å) for a shorter period of time, it was considered to be transiently inserted into the S2 site. In this scenario, the interactions between the detergent and S2 site residues were forming and breaking dynamically (e.g., Figure 5). Finally, if d_{min} > 5 Å at all times during the trajectory, then the LeuT molecule was not considered to be penetrated by DDM.

RESULTS

DDM Molecules Form a Converged Shell around LeuT. To determine the behavior of the DDM molecule number in a micellar system surrounding LeuT, we conducted MD studies on a series of LeuT-DDM complexes constructed to explore systematically the effect of protein-to-detergent (P/D) number ratios on the nature and dynamics of the resulting complexes. The MD simulations of the systems containing from 1:160 (low detergent content) to 1:300 (high detergent content) P/D ratios, starting from the constructs described as starting configurations in Figure 1 in which various numbers of monomeric DDM molecules were added randomly outside the protein/micelle complex (Figures 1 and 2A,B). The various constructs converged (at the simulation times indicated) to configurations with very similar DDM shells (defined in Methods as the shell) surrounding the protein. Specifically, as shown in Figure 3, we found that in all of the simulations the number of detergent molecules in the shell was ∼120. (See also Figure 2D.) We note that the convergence of the DDM numbers in the shell to similar values in the different simulations is independent of the range explored specifically, from 3 to 5 Å (Figure S1 in the Supporting Information).

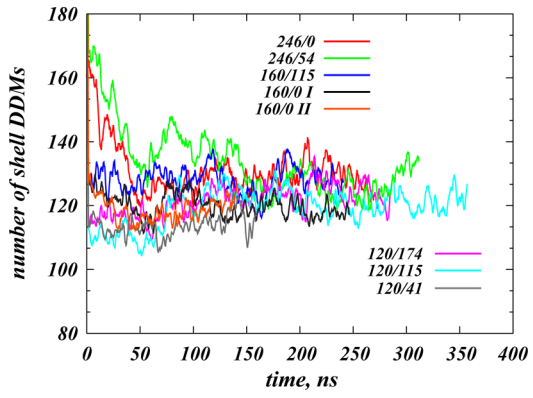

Figure 3. Time evolution (after initial equilibration phase) of the number of DDM molecules within 4 Å of the protein (i.e., shell) in different simulations. The traces were smoothed by the running average algorithm.

To investigate further the stability of the identified shell, a second set of MD simulations was carried out as defined in resulting configurations (Figure 1). The starting constructs were obtained by extracting LeuT with its shell DDM molecules (120 detergents) from a representative snapshot from the starting configurations trajectories and surrounding this complex with different numbers of monomeric DDMs. MD trajectories that were 200−350 ns long were collected in the environment defined in Methods. As illustrated in Figure 3, this second set of MD simulations also converged to configurations in which the shell surrounding LeuT contained ∼120 DDM molecules. These results suggest that irrespective of the P/D ratio a converged shell of DDMs forms around LeuT. Interestingly, however, quantitative analysis of various types of detergent aggregates forming in the MD trajectories revealed that the detergent aggregation number, i.e. the number of DDM molecules comprising the entire micelle enclosing LeuT (denoted as DM in Methods) strongly depends on the P/D ratio.

Formation and Dynamics of Various DDM Aggregates around LeuT. Figure 4A shows the average number of DDM molecules in the entire micelle surrounding LeuT (DM) as well as in aggregates bound to DM (BM and BA) and in the entire complex of detergent associated with the central protein/micelle complex (i.e., DM, BM, and BA together, which is the proteomicelle aggregation number). The averages were obtained from the analysis of the last 50 ns of each trajectory. The time trace in Figure 4B illustrates the evolution of these aggregates from one particular 160/115 simulation, and Figure 4C shows, from the same simulation, the evolution of DDM numbers in the free aggregates compared to that in the central protein/micelle. (Analogous plots for other constructs can be found in Figures S2−S3 in the Supporting Information.)

The results in Figure 4C show that over 80% of 275 DDMs present in the 160/115 system become part of the central micelle (blue line in Figure 4C). The majority of the detergent that is still in the solution assembles spontaneously into free aggregates (FAs, red line in Figure 4C), whereas free monomers (FMs) practically disappear (black line in Figure 4C). The interconversion of the different bound aggregates (BA and BM) and their melting into the central DM that surrounds LeuT are illustrated in Figure 4B. Thus, within the first 50 ns, the number of DDMs in DM increases from ∼160 to ∼190 and remains at this level until the 100 ns time point (red trace in Figure 4B). At the same time, the number of aggregates bound to DM remains more or less unchanged (green trace in Figure 4B). Interestingly, in the subsequent 100−150 ns time interval we observe a sudden increase in the number of detergent molecules in DM as a result of the fusion of the bound aggregates with the central micelle (green curve in Figure 4B decreases to ∼0). After the fusion process is completed (∼150 ns), the detergent count in DM and in DM + BA + BM remains nearly identical for the remainder of the trajectory (red and blue traces in Figure 4B), indicating that practically all bound aggregates (over 80% of the DDM, see Figure 4C, blue curve) become part of the DM.

Although the size of the DDM shell appears to be ∼120 DDM (as calculated at a 4 Å distance cutoff) regardless of the P/D ratio, we found the aggregation number to change significantly in the P/D interval of 1:246 to 1:300 interval, from 204±5 (in the 120/174 simulation) to 243±7 (for the 246/54

dx.doi.org/10.1021/ja405984v | J. Am. Chem. Soc. 2013, 135, 14266−14275

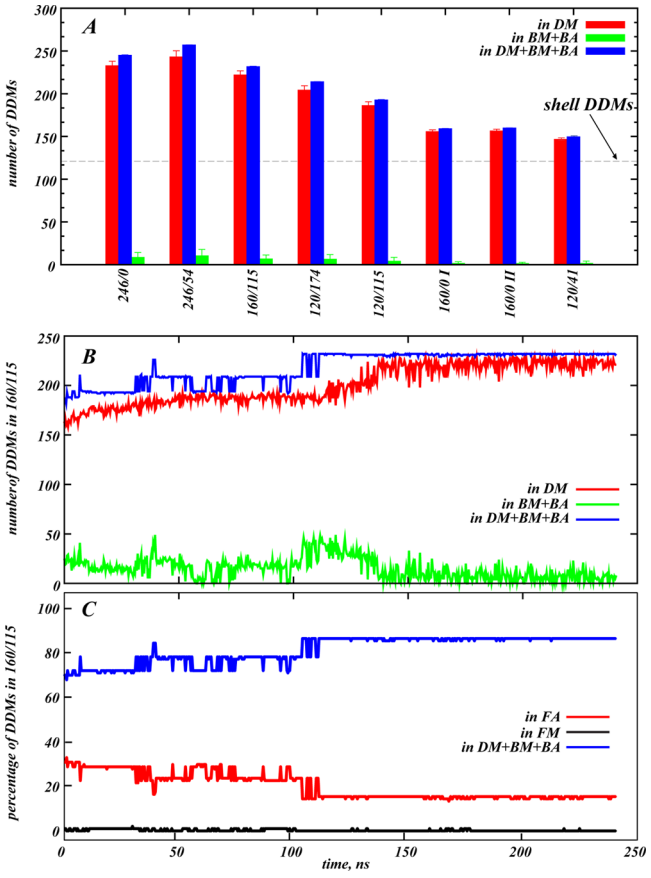

Figure 4. (A) Average number of DDM molecules in the detergent micelle around LeuT (DM), in the aggregates bound to DM (BA and BM), and in DM, BA, and BM taken together. For each simulated system, the averages were calculated using the last 50 ns segments of the respective trajectories. The dashed horizontal line indicates the average number of DDMs (~120) in the detergent shell around LeuT established from Figure 3. (B) Time evolution (after initial equilibration phase) of the measures from panel A in the 160/115 simulation. (C) Percentage of DDM detergents in DM, BA, and BM (blue line), in FA (red line), and in FM (black line) as a function of time in the 160/115 simulation. For definitions of the various types of aggregates, see Methods.

system), as seen in Figure 4A. Moreover, these values are substantially higher than the 145±3 to 156±2 aggregation number range that we find for the three different simulations under low detergent condition (1:160 P/D ratio). Indeed, our results suggest that for the low DDM constructs all of the available detergent eventually aggregates with the central DM around the protein. Interestingly, at an intermediate P/D ratio of 1:235, the aggregation number (186±5) is in between these two regimes.

We note that the extensive simulation times that we have reached in the current studies still may not be sufficient for complete equilibration of the dynamic variables discussed in Figure 4A (Figures 4B,C and S2−S5 in the Supporting Information). However, the examination of a number of control trajectories for the high detergent regime (Figure 1 flowchart) allowed us to assess with confidence the convergence of the aggregation numbers from below (120/174, 120/115, and 160/115 simulations) as well as from above (246/0 and 246/54 simulations). On the basis of the average values from these simulations initiated from different starting conditions (Figure 4A), we therefore conclude that for the high detergent regime the DDM aggregation number around LeuT is 226±17. In the low DDM regime, such as the P/D ratio of 1:160, our results suggest that all available detergents will constitute the DM.

Detergent Penetration into LeuT Is Dependent on the Aggregation Number of DDMs around the Transporter: Two Distinct Pathways for Detergent Penetration. In the course of simulations with some of the constructs, we observed DDM molecules inserting into LeuT. The penetration was gradual and in some cases transient. However, when a stable complex was formed, the single DDM molecule penetrated the LeuT molecule until it ended up interacting with residues in the identified "extracellular vestibule" of LeuT, the "S2 site."[19,29] (see below.) Such complete DDM penetration occurred only in the constructs with relatively high detergent content, i.e. for P/D ratios in the 1:246 to 1:300 range (Table 1). In contrast, only transient DDM insertion into LeuT was observed in simulations of systems with low (1:160 P/D ratio) or intermediate (1:235 P/D ratio) detergent content. We identified two alternative pathways for DDM insertion into LeuT, one termed "from the side" penetration and the other termed "from the top" penetration (Table 1).

Table 1. Occurrence of Detergent Penetration of LeuT in Various Simulations

	detergent penetration mode[a]	
simulations	from the side	from the top
246/54[b]	complete	complete
120/174	transient	complete
160/115	complete	no
246/0	transient	complete
120/115	transient	no
120/41	no	no
160/0 I	no	transient
160/0 II	transient	no

[a]For the definition of different modes of detergent penetration, see Results. [b]Different simulations are labeled as A/B, where A and B represent the initial number of DDM molecules in the micelle and in solution, respectively. (See also Figure 1.)

The "from the side" penetration was observed in several of the MD simulations (Table 1), and the path is illustrated in Figure 5 for the 160/115 construct. The DDM molecule enters the transporter through an area between the extracellular (EC) ends of TMH11 and TMH6. The first contacts established by the DDM molecule involve residues Pro241, Gly242, and Ile245 in TMH6, Trp467, and Val466 in TMH11 (Figure S4 in the Supporting Information). As it penetrates deeper into the transporter, the detergent molecule engages in additional strong interactions with Phe405 in TMH10 (Figure S3) and eventually with Gln34 and Arg30 in TMH1 (Figure 5C,D). The participation of the latter two residues is especially intriguing because both Gln34 and Arg30 are situated in the functionally important S2 site of LeuT.[19,29] As seen in Figure 5A,B, the DDM is stabilized in the S2 site through both hydrophobic and polar interactions as the DDM headgroup engages with the Arg30-Gln34 pair whereas the tail interacts with hydrophobic residues lining the EC ends of TMH6 and TMH11. Notably, this entry pathway and the identity of residues participating in interactions with the detergent were

dx.doi.org/10.1021/ja405984v | J. Am. Chem. Soc. 2013, 135, 14266−14275

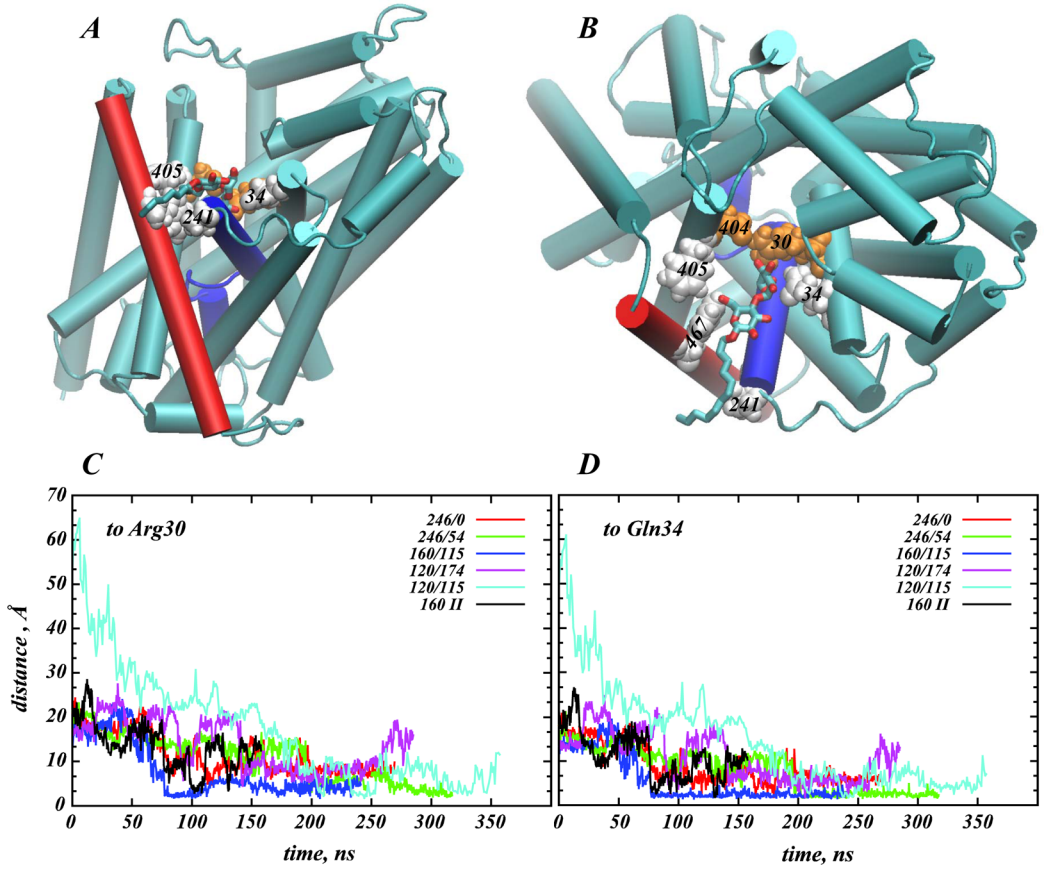

Figure 5. From the side entry pathway of a DDM molecule into LeuT. (A, B) Representative snapshot from the 160/115 simulation showing DDM detergent (in licorice) penetrating LeuT (in cartoon). TMH6 and TMH11 of the transporter are colored blue and red, respectively, and the key residues are shown in a space-filled representation and are labeled. (C, D) Time traces of the minimal distance from the inserted detergent molecule to Arg30 (panel D) and to Gln34 (panel C) in 246/54, 160/115, and 120/115 trajectories.

found to be remarkably consistent among these different simulations, although the extent of the detergent penetration in these trajectories (Figure 5C,D and also Methods for insertion criteria) ranged from completely inserted (in the 160/115 and 246/54 systems) to transiently bound (120/115, 246/0, 120/174, and 160/0 II simulations).

Penetration from the top of the transporter was observed in the 246/54, 120/174, and 160/0 I simulations (Table 1). The initial contact was observed to involve the Phe235-Asp240 stretch of EC loop 3 (ECL3), and the insertion proceeded toward the Gly307-Ala317 segment in ECL4 (Figure S5 in the Supporting Information). As the DDM molecule penetrated with its headgroup deeper into the transporter, the final set of stabilizing interactions included Phe320 in ECL4 and Leu400 in TMH10 (Figure 6). The participation of these particular residues in interactions with the inserted detergent is important because they are again, as in the from the side penetration, situated in the functionally important S2 site and Leu400 has been directly linked to the functional mechanisms of substrate transport through LeuT.[19,29]

An interesting variation on the mode of binding is observed in the 246/0 trajectory where the inserted detergent molecule is engaged in stabilizing interactions with the same residues as identified in the simulations of the 246/54, 120/174, and 160/0 I constructs (Figure 6C,D), but it is the hydrocarbon tail that interacts with Phe320 and Leu400 residues rather than its headgroup atoms (cf. Figure 6A,B).

The convergence of penetration paths and stabilization sites from the various simulations with different constructs indicates the robust nature of these conclusions. Moreover, we note that in two trajectories (246/54 and 120/174) in which the detergent entered the protein from the top, the specific DDM molecule that eventually ended in the S2 site of LeuT came from outside the protein-surrounding micelle, from among those in the monomeric form (data not shown). Similarly, the DDM molecule that entered S2 site from the side in the 120/115 simulation (Figure 5C,D) inserted itself into the protein after diffusing toward LeuT from the solution. These trends suggest that the MD simulations were sufficiently long to allow DDM molecules to diffuse over relatively long distances before reaching the binding sites in the transporter.

■ DISCUSSION

The dependence of specific measurable properties of LeuT on the quantitative parameters of the micellar system offers the first detailed molecular perspective on the manner in which detergent solubilization can affect functional phenotypes of this type of membrane protein. The insights result from extensive atomistic MD simulations of different regimes of protein-to-detergent number ratios that are commonly used to prepare protein for biochemical/biophysical studies and crystallography. This study followed our recent work[19] that highlighted the effect of the experimental conditions on the activity of LeuT, in particular, how high DDM concentrations can obscure substrate binding to the functionally important S2 site. Taken

dx.doi.org/10.1021/ja405984v | J. Am. Chem. Soc. 2013, 135, 14266−14275

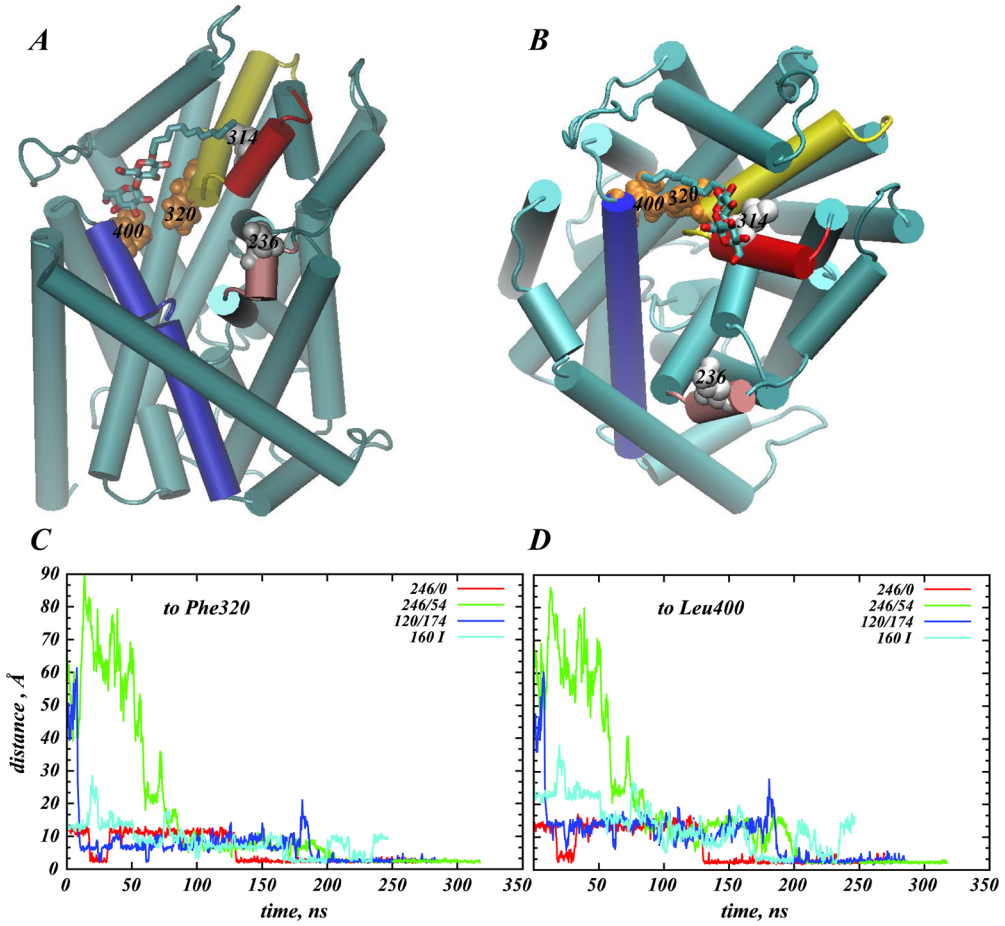

Figure 6. From the top entry pathway of DDM molecule into LeuT. (A, B) Representative snapshots from the 246/54 (A) and the 246/0 (B) simulations showing DDM detergent (in licorice) penetrating LeuT (in cartoon). Different segments of the transporter are highlighted as follows: TMH10 (blue), 235−240 stretch in ECL3 (pink), 307−316 in ECL4 (red), and 317−336 (yellow). Glu236 and Ile314 are shown by the white space fill, and Phe320 and Leu400 are depicted by the orange space fill. (C, D) Time traces of the minimal distance from the inserted detergent molecule to Phe320 (panel C) and to Leu400 (panel D) in 246/0, 246/54, and 120/174 simulations.

together, our studies indicate that DDM at high concentrations can occupy the S2 site in LeuT, just like OG.[21] These studies emphasize the sensitivity of the S2 site, a site that is yet to be identified with crystallographic approaches in a substrate-occupied state. Because the crystallization of membrane proteins requires high protein concentrations that are routinely obtained with centrifugal filtration of purified material in protein−detergent mixtures, our studies emphasize a common problem that is associated with the use of protein in detergent-solubilized form. A key observation of the present study is the formation of a converged shell around LeuT established irrespective of detergent concentration (within the wide range explored in our studies). This nucleus of detergent molecules effectively protects the transporter TM segments from unfavorable hydrophobic/hydrophilic exposure and therefore is key to the stability of the protein. Indeed, in control simulations initiated with a nucleus of 100 DDM molecules surrounding LeuT, the system exhibited instabilities during the trajectory, which resulted in substantial water penetration of the hydrophobic core of the transporter (data not shown). Taken together, our findings establish the importance of considering DDM-to-protein number ratios at or above ∼120 in MD simulations of LeuT proteomicelles (i.e., the number required for the formation of a converged shell at 4 Å radius).

It is not surprising given the shape of the protein that our simulations show that the proteomicelles forming around LeuT are nonspherical in shape (Figure S6 in the Supporting Information). The aggregation number of DDM in the micelle that surrounds the transporter depends strongly on the P/D ratio (Figure 4A). Specifically, in the high DDM concentration regime we identified 226±17 detergent molecules in the protein-solubilizing micelle, which is significantly larger than the usual aggregation number for DDM in micelles (∼140);[49] for low detergent content (P/D ratio of 1:160), our results indicate the aggregation of all of the available detergent into the LeuT-binding micelle. We note that the calculated proteomicelle aggregation number (226±17) is not dependent on the simulation box size because there always will exist, irrespective of the available volume, partially formed detergent micelles in the solution together with protemicelles, as observed in our simulations.

Remarkably, the penetration of a DDM molecule that inserts fully into the transporter, whether it follows the from the top or from the side path described in the Results of the MD simulations, is found to occur only in the constructs with high detergent content (P/D ratio range of 1:246 to 1:300); any penetration observed in systems with low or intermediate DDM fraction is at most transient. Because the shell surrounding LeuT does not depend on the detergent

dx.doi.org/10.1021/ja405984v | J. Am. Chem. Soc. 2013, 135, 14266−14275

concentration and it is the DDM aggregation number for the system (and thus the protein-to-detergent number ratio) that determines penetration, it becomes clear that DDM insertion into LeuT is not simply related to the interaction with the detergent immediately surrounding the transporter. Rather, it reflects the dynamic properties of the detergent in the system. Specifically, we reason that at low detergent concentrations (at or below 226±17 aggregation number established by our studies) all of the DDM molecules in the system are expected to participate in the stabilization of the proteomicelle. But at higher concentrations, excess DDMs, not associated with the proteomicelle, will be present in the solution and will diffuse freely in monomeric and/or in aggregate forms. Such dynamics of free detergent increases the probability of random encounters with the protein regions exposed to the solvent and specifically with the large extracellular vestibule of LeuT, which eventually leads to the observed detergent penetration.

The final position of any completely penetrating DDM was found to be the S2 site in the extracellular vestibule of LeuT and to involve Arg30, Gln34, Phe320, and Leu400 in strong interactions with the inserted DDM. These residues have been identified to have functional importance in the transport mechanism. Specifically, in crystal structures of LeuT these residues are among those implicated in stabilizing interactions with tricyclic antidepressants (TCAs) in the extracellular vestibule[25] as well as with OG detergent[21] and to bind inhibitors (such as Trp).[24] Furthermore, highly conserved ionic interactions between Arg30 and Asp404 in TMH10 have been established as one of the structural/functional hallmarks in NSS family proteins that regulate the access of the substrate from the EC vestibule down to the S1 site during the transport cycle.[20,29,50] In addition, the importance of Leu400 residue in the LeuT function is highlighted by the phenotypes of Leu400-to-Ser or Leu400-to-Cys mutations that impair Leu substrate binding in the S2 site.[19]

Notably, detergent penetration events observed in the simulations occur at P/D ratios that are expected to be realized in the local environments of the solubilized LeuT proteins during in vitro experiments. Thus, the results from the simulations presented here correspond to the experimental observation[19] that the binding of the Leu substrate at the S2 site is impaired if LeuT is preincubated in the presence of high DDM (0.3%), yielding a protein-to-detergent ratio of ∼1:225, but this does not occur at low DDM concentrations (0.1%, with a protein-to-detergent ratio of ∼1:170). A detailed scan through the detergent concentration range revealed that the loss of Leu binding occurs abruptly in the interval between 0.15 and 0.175% DDM concentration.[19] In qualitative agreement with these experimental observations, our data indicate the existence of two distinct regimes for DDM concentration, separated by a narrow range of P/D ratios (from 1:235 to 1:246), that determine detergent penetration. This suggests a mechanistic explanation for the experimentally observed impairment of the S2 site under high detergent conditions that involves the steric hindrance of the S2 site by a penetrating DDM molecule, much like the proposed effect of OG on LeuT when bound in the S2 site.[21] In the low detergent concentration regime, our results suggest that DDM molecules penetrate LeuT only transiently, therefore leaving the S2 site more accessible for substrate binding. Importantly, we stress that because even at the lowest P/D ratios studied here (1:160) the detergent can still penetrate LeuT (albeit transiently) and given the narrow P/D ratio range that determines the extent of detergent insertion, the data and hypothesis presented above provide a plausible explanation for the findings from the recent functional experiments on LeuT[28] that were interpreted to suggest the existence of only a single high-affinity S1 site even at low detergent concentrations. Furthermore, the results presented here illustrate, on the molecular level, how even small variations in protein preparation with detergent can lead to the differential behavior of the proteomicelle and to differences in processes such as the penetration of detergent into the transporter. Such differences have potentially quite different outcomes in measurements of protein function.

We note that to establish unambiguously the conditions concerning DDM penetration behavior and protection by lipids it becomes essential to expand the current MD simulations to more complex environments that involve mixed phospholipid-detergent micelles. This is because the treatment of the protein with detergent generally retains a relatively small annulus of lipid molecules that are being extracted together with the protein during the solubilization process. This annulus of lipids can be expected to create a new set of local interactions with the protein and with the detergent, and these could affect the detergent penetration (especially from the side) of LeuT. To establish the specific conditions regarding the lipid core, we are currently extending the studies of LeuT in mixed micelles by probing different simulation conditions, and the results will be presented in a subsequent publication.

■ ASSOCIATED CONTENT

Supporting Information

Number of detergent molecules, volumes, and molar concentrations of the detergent in the simulated systems. DMM molecule penetration. Time evolution of the number of DDM molecules under various conditions. Characterization of micelle shape. This material is available free of charge via the Internet at http://pubs.acs.org.

■ AUTHOR INFORMATION

Corresponding Author

gek2009@med.cornell.edu

Notes

The authors declare no competing financial interest.

■ ACKNOWLEDGMENTS

We acknowledge stimulating discussions with Sayan Mondal. G.K. is grateful to Helgi Ingolfsson for advice on setting up detergent micelle constructs around LeuT. This work was supported by National Institutes of Health grants P01DA012408, R01DA17293, K05DA022413, and U54GM087519. M.L. was supported by the National Institutes of Health under Ruth L. Kirschstein National Research Service Award F31DA035533. Computational resources were provided by Teragrid allocation MCB120008 on the Ranger and Stampede machines, by the NERSC allocation m1710 on the Carver cluster, and by the Institute for Computational Biomedicine at Weill Cornell Medical College of Cornell University.

■ REFERENCES

(1) Andersen, O. S.; Koeppe, R. E. *Annu. Rev. Biophys. Biomol. Struct.* **2007**, *36*, 107−130.
(2) Dart, C. *J. Physiol.* **2010**, *588*, 3169−3178.
(3) McIntosh, T. J.; Simon, S. A. *Annu. Rev. Biophys. Biomol. Struct.* **2006**, *35*, 177−198.

(4) Marsh, D. *Biochim. Biophys. Acta* **2008**, *1778*, 1545−1575.
(5) Lingwood, D.; Simons, K. *Science* **2010**, *327*, 46−50.
(6) Staubach, S.; Hanisch, F. G. *Exp. Rev. Proteomics* **2011**, *8*, 263−277.
(7) Han, Y.; Moreira, I. S.; Urizar, E.; Weinstein, H.; Javitch, J. A. *Nat. Chem. Biol.* **2009**, *5*, 688−695.
(8) Huang, P.; Xu, W.; Yoon, S. I.; Chen, C.; Chong, P. L.; Liu-Chen, L. Y. *Biochem. Pharmacol.* **2007**, *73*, 534−549.
(9) Xu, W.; Yoon, S. I.; Huang, P.; Wang, Y.; Chen, C.; Chong, P. L.; Liu-Chen, L. Y. *J. Pharmacol. Exp. Ther.* **2006**, *317*, 1295−1306.
(10) Pontier, S. M.; Percherancier, Y.; Galandrin, S.; Breit, A.; Gales, C.; Bouvier, M. *J. Biol. Chem.* **2008**, *283*, 24659−24672.
(11) Boesze-Battaglia, K.; Hennessey, T.; Albert, A. D. *J. Biol. Chem.* **1989**, *264*, 8151−8155.
(12) Mondal, S.; Khelashvili, G.; Shan, J.; Andersen, O. S.; Weinstein, H. *Biophys. J.* **2011**, *101*, 2092−2101.
(13) Shan, J.; Khelashvili, G.; Mondal, S.; Mehler, E. L.; Weinstein, H. *PLoS Comput. Biol.* **2012**, *8*, e1002473.
(14) Simons, K.; Ikonen, E. *Nature* **1997**, *387*, 569−572.
(15) Cremona, M. L.; Matthies, H. J.; Pau, K.; Bowton, E.; Speed, N.; Lute, B. J.; Anderson, M.; Sen, N.; Robertson, S. D.; Vaughan, R. A.; Rothman, J. E.; Galli, A.; Javitch, J. A.; Yamamoto, A. *Nat. Neurosci.* **2011**, *14*, 469−477.
(16) Seddon, A. M.; Curnow, P.; Booth, P. J. *Biochim. Biophys. Acta* **2004**, *1666*, 105−117.
(17) Lichtenberg, D.; Opatowski, E.; Kozlov, M. M. *Biochim. Biophys. Acta* **2000**, *1508*, 1−19.
(18) Dodes Traian, M. M.; Cattoni, D. I.; Levi, V.; Gonzalez Flecha, F. L. *PLoS One* **2012**, *7*, e39255.
(19) Quick, M.; Shi, L.; Zehnpfennig, B.; Weinstein, H.; Javitch, J. A. *Nat. Struct. Mol. Biol.* **2012**, *19*, 207−211.
(20) Gether, U.; Andersen, P. H.; Larsson, O. M.; Schousboe, A. *Trends Pharmacol. Sci.* **2006**, *27*, 375−383.
(21) Quick, M.; Winther, A. M.; Shi, L.; Nissen, P.; Weinstein, H.; Javitch, J. A. *Proc. Natl. Acad. Sci. U.S.A* **2009**, *106*, 5563−5568.
(22) Krishnamurthy, H.; Gouaux, E. *Nature* **2012**, *481*, 469−474.
(23) Piscitelli, C. L.; Gouaux, E. *EMBO J.* **2012**, *31*, 228−35.
(24) Singh, S. K.; Piscitelli, C. L.; Yamashita, A.; Gouaux, E. *Science* **2008**, *322*, 1655−61.
(25) Singh, S. K.; Yamashita, A.; Gouaux, E. *Nature* **2007**, *448*, 952−956.
(26) Wang, H.; Elferich, J.; Gouaux, E. *Nat. Struct. Mol. Biol.* **2012**, *19*, 212−219.
(27) Yamashita, A.; Singh, S. K.; Kawate, T.; Jin, Y.; Gouaux, E. *Nature* **2005**, *437*, 215−223.
(28) Wang, H.; Gouaux, E. *EMBO Rep.* **2012**, *13*, 861−866.
(29) Shi, L.; Quick, M.; Zhao, Y.; Weinstein, H.; Javitch, J. A. *Mol. Cell* **2008**, *30*, 667−677.
(30) Kasimova, A. O.; Pavan, G. M.; Danani, A.; Mondon, K.; Cristiani, A.; Scapozza, L.; Gurny, R.; Moller, M. *J. Phys. Chem. B* **2012**, *116*, 4338−4345.
(31) Bond, P. J.; Cuthbertson, J.; Sansom, M. S. *Biochem. Soc. Trans.* **2005**, *33*, 910−912.
(32) Bond, P. J.; Cuthbertson, J. M.; Deol, S. S.; Sansom, M. S. *J. Am. Chem. Soc.* **2004**, *126*, 15948−15949.
(33) Bond, P. J.; Holyoake, J.; Ivetac, A.; Khalid, S.; Sansom, M. S. *J Struct Biol* **2007**, *157*, 593−605.
(34) Bond, P. J.; Sansom, M. S. *J. Mol. Biol.* **2003**, *329*, 1035−1053.
(35) Khalid, S.; Bond, P. J.; Carpenter, T.; Sansom, M. S. *Biochim. Biophys. Acta* **2008**, *1778*, 1871−1880.
(36) Psachoulia, E.; Bond, P. J.; Sansom, M. S. *Biochemistry* **2006**, *45*, 9053−9058.
(37) Ingolfsson, H. I.; Li, Y.; Vostrikov, V. V.; Gu, H.; Hinton, J. F.; Koeppe, R. E., II; Roux, B.; Andersen, O. S. *J. Phys. Chem. B* **2011**, *115*, 7417−7426.
(38) Patargias, G.; Bond, P. J.; Deol, S. S.; Sansom, M. S. *J. Phys. Chem. B* **2005**, *109*, 575−582.
(39) Friemann, R.; Larsson, D. S.; Wang, Y.; van der Spoel, D. *J. Am. Chem. Soc.* **2009**, *131*, 16606−16607.
(40) Sali, A.; Blundell, T. L. *J. Mol. Biol.* **1993**, *234*, 779−815.
(41) Shaikh, S. A.; Tajkhorshid, E. *PLoS Comput. Biol.* **2010**, *6*.
(42) Zhao, C.; Stolzenberg, S.; Gracia, L.; Weinstein, H.; Noskov, S.; Shi, L. *Biophys. J.* **2012**, *103*, 878−88.
(43) le Maire, M.; Champeil, P.; Moller, J. V. *Biochim. Biophys. Acta* **2000**, *1508*, 86−111.
(44) Kaufmann, T. C.; Engel, A.; Remigy, H. W. *Biophys. J.* **2006**, *90*, 310−317.
(45) Phillips, J. C.; Braun, R.; Wang, W.; Gumbart, J.; Tajkhorshid, E.; Villa, E.; Chipot, C.; Skeel, R. D.; Kale, L.; Schulten, K. *J. Comput. Chem.* **2005**, *26*, 1781−1802.
(46) Brooks, B. R.; Brooks, C. L., III; Mackerell, A. D., Jr.; Nilsson, L.; Petrella, R. J.; Roux, B.; Won, Y.; Archontis, G.; Bartels, C.; Boresch, S.; Caflisch, A.; Caves, L.; Cui, Q.; Dinner, A. R.; Feig, M.; Fischer, S.; Gao, J.; Hodoscek, M.; Im, W.; Kuczera, K.; Lazaridis, T.; Ma, J.; Ovchinnikov, V.; Paci, E.; Pastor, R. W.; Post, C. B.; Pu, J. Z.; Schaefer, M.; Tidor, B.; Venable, R. M.; Woodcock, H. L.; Wu, X.; Yang, W.; York, D. M.; Karplus, M. *J. Comput. Chem.* **2009**, *30*, 1545−1614.
(47) Abel, S.; Dupradeau, F. Y.; Raman, E. P.; MacKerell, A. D., Jr.; Marchi, M. *J Phys Chem B* **2011**, *115*, 487−499.
(48) Essmann, U.; Perera, L.; Berkowitz, M. L.; Darden, T.; Lee, H.; Pedersen, L. G. *J. Chem. Phys.* **1995**, *103*, 8577−8593.
(49) Tummino, P. J.; Gafni, A. *Biophys. J.* **1993**, *64*, 1580−1587.
(50) Shan, J.; Javitch, J. A.; Shi, L.; Weinstein, H. *PLoS One* **2011**, *6*, e16350.